



Article

Genome-Wide Identification and Expression Analysis of *AMT* and *NRT* Gene Family in Pecan (*Carya illinoensis*) Seedlings Revealed a Preference for NH_4^+ -N

Mengyun Chen ^{1,2}, Kaikai Zhu ^{1,2} , Junyi Xie ^{2,3} , Junping Liu ^{1,2}, Pengpeng Tan ^{1,2} and Fangren Peng ^{1,2,*}

¹ Co-Innovation Center for Sustainable Forestry in Southern China, College of Forestry, Nanjing Forestry University, Nanjing 210037, China

² College of Forestry, Nanjing Forestry University, Nanjing 210037, China

³ Department of Ecology, Nanjing Forestry University, Nanjing 210037, China

* Correspondence: frpeng@njfu.edu.cn; Tel.: +86-25-8542-7995

Abstract: Nitrogen (N) is a major limiting factor for plant growth and crop production. The use of N fertilizer in forestry production is increasing each year, but the loss is substantial. Mastering the regulatory mechanisms of N uptake and transport is a key way to improve plant nitrogen use efficiency (NUE). However, this has rarely been studied in pecans. In this study, 10 *AMT* and 69 *NRT* gene family members were identified and systematically analyzed from the whole pecan genome using a bioinformatics approach, and the expression patterns of *AMT* and *NRT* genes and the uptake characteristics of NH_4^+ and NO_3^- in pecan were analyzed by aeroponic cultivation at varying $\text{NH}_4^+/\text{NO}_3^-$ ratios (0/0, 0/100, 25/75, 50/50, 75/25, 100/0 as CK, T1, T2, T3, T4, and T5). The results showed that gene duplication was the main reason for the amplification of the *AMT* and *NRT* gene families in pecan, both of which experienced purifying selection. Based on qRT-PCR results, *CiAMTs* were primarily expressed in roots, and *CiNRTs* were majorly expressed in leaves, which were consistent with the distribution of pecan NH_4^+ and NO_3^- concentrations in the organs. The expression levels of *CiAMTs* and *CiNRTs* were mainly significantly upregulated under N deficiency and T4 treatment. Meanwhile, T4 treatment significantly increased the NH_4^+ , NO_3^- , and NO_2^- concentrations as well as the V_{max} and K_m values of NH_4^+ and NO_3^- in pecans, and V_{max}/K_m indicated that pecan seedlings preferred to absorb NH_4^+ . In summary, considering the single N source of T5, we suggested that the $\text{NH}_4^+/\text{NO}_3^-$ ratio of 75:25 was more beneficial to improve the NUE of pecan, thus increasing pecan yield, which provides a theoretical basis for promoting the scale development of pecan and provides a basis for further identification of the functions of *AMT* and *NRT* genes in the N uptake and transport process of pecan.



Citation: Chen, M.; Zhu, K.; Xie, J.; Liu, J.; Tan, P.; Peng, F. Genome-Wide Identification and Expression Analysis of *AMT* and *NRT* Gene Family in Pecan (*Carya illinoensis*) Seedlings Revealed a Preference for NH_4^+ -N. *Int. J. Mol. Sci.* **2022**, *23*, 13314. <https://doi.org/10.3390/ijms232113314>

Academic Editor: Xiao-Fei Wang

Received: 30 August 2022

Accepted: 28 October 2022

Published: 1 November 2022

Publisher's Note: MDPI stays neutral with regard to jurisdictional claims in published maps and institutional affiliations.



Copyright: © 2022 by the authors. Licensee MDPI, Basel, Switzerland. This article is an open access article distributed under the terms and conditions of the Creative Commons Attribution (CC BY) license (<https://creativecommons.org/licenses/by/4.0/>).

Keywords: NH_4^+ ; NO_3^- ; *AMT*; *NRT*; pecan

1. Introduction

Ammonium nitrogen (NH_4^+) and nitrate nitrogen (NO_3^-) are the two main forms of nitrogen (N) that plants can absorb and use. The absorption, transport, and assimilation of NH_4^+ and NO_3^- in plants have been studied extensively. Physiologically, NH_4^+ and NO_3^- uptake and translocation systems were identified mainly by root absorption kinetics, which were classified into two types: high-affinity transport systems (HATs) and low-affinity transport pathways (LATs) [1]. V_{max} (maximum ion uptake rate) and K_m (Mie's constant) are the two main parameters in the kinetic equation for root nutrient uptake, which can quantitatively characterize the plant uptake of nutrient ions. In general, a larger V_{max} value indicates that the plant has a great uptake potential for a certain ion, and the number of the ion transport carrier protein on the cell membrane determines the size of V_{max} . K_m indicates the affinity between the ion absorbed by the root system and the uptake site (transport carrier), and the greater the affinity, the smaller the K_m value [2]. Previous

studies have found that plants have a preference for the intake and utilization of NH_4^+ and NO_3^- ; when both N forms are present, plants will preferentially intake and utilize one of them [3]. At the molecular level, many members of the ammonium transporter (AMT) and nitrate transporter (NRT) gene families have been cloned and characterized, and the uptake and utilization of NH_4^+ and NO_3^- by plants is regulated by multiple genes in the N transporter protein family [4,5].

AMTs are carrier proteins that actively transport NH_4^+ across biological cell membranes, and they were divided into three main subfamilies: AMT/MEP/Rh (Ammonium transporter/Methylamine permease/Rhesus protein) [6]. The AMT family can usually be divided into two subfamilies, namely AMT1 and AMT2 [7]. Both AMT1 and AMT2 show high affinity for NH_4^+ , but members of the AMT1 subfamily play a more important role in high-affinity NH_4^+ uptake [8]. AMT2 has a more complex gene structure and protein profile than AMT1 [9]. The AMT1 subfamily of *Arabidopsis thaliana* has five members, while AMT2 has low homology with the five AMT1 subfamily members and belongs to the MEP subfamily [10]. Expression of *AtAMT1;1* in roots is significantly correlated with N uptake, whereas expression of *AtAMT1;2* in roots is insensitive to changes in N concentration [11]. *AtAMT1;4* mediate the intake of NH_4^+ at the pollen plasma membrane [12]. NH_4^+ is regulated into the cytoplasm through *AtAMT1;1* and *AtAMT2;1*, which are primarily expressed in leaves [13]. In addition, *AtAMT2;1* may play a role in the transport of NH_4^+ from the roots to the ground [10]. A study by Couturier et al. on AMT proteins in poplar (*Populus L.*) found that the expression of *PtrAMT1;2* was influenced by intracellular N concentration. Most *PtrAMT1*s were preferentially expressed in roots, while most *PtrAMT2*s were majorly expressed in stems, and *PtrAMT3;1* was expressed only in senescing leaves [14].

The absorption systems, corresponding genes, and regulatory mechanisms of NO_3^- by plants are different from those of NH_4^+ . The uptake of NO_3^- by plants is the process of pumping protons out of the cell through the H^+ -ATPase in the plasma membrane, creating pH and electrical ($\Delta\Psi$) gradients across the plasma membrane that allows the NO_3^- transporter to take up NO_3^- into the cell [15]. Four families of transporters are known to contribute to nitrate uptake and transport in plants: the nitrate transporter protein 1 (NRT1/PTR/NPF), nitrate transporter 2 (NRT2), chloride channel (CLC), and slow anion-associated channel homolog (SLC/SLAH) family [16]. The NRT1 and NRT2 are responsible for LATS and HATS, respectively [17]. Members of the NRT1 subfamily are responsible for transporting NO_3^- , hormones, glucosinolates and dipeptides [18]. In *Arabidopsis*, *AtNPF6;3/AtNRT1;1/CHL1* was the first NRT1 subfamily member to be identified and cloned, and this protein is an amphiphilic NRT [19]. Except for *AtNRT1;1*, most NRT1 exhibited low affinity [20]. *NPF4;6/NRT1;2* and *NPF2;7/NAXT1* were also shown to be involved in root NO_3^- uptake, with *NPF4.6* acting on NO_3^- influx [21] and *NPF2.7* involved in NO_3^- efflux [22]. Other NRT1s are mainly related to the internal transport of NO_3^- in processes such as xylem and phloem loading and transport to leaves or seeds [23]. NRT2 belongs to the major facilitator superfamily (MFS) [24], NRT3/NAR2 is a high-affinity NRT [25]. *NRT2.1*, *NRT2.2*, *NRT2.4*, and *NRT2.5* were known to be associated with root NO_3^- influx, and *AtNRT2.1* expression was induced at low NO_3^- levels and repressed at high NO_3^- concentrations [26]. *AtNRT2.4* and *AtNRT2.5* are associated with root NO_3^- absorbance during severe N deficiency [27]. The NRT3 subfamily plays a significant role in NO_3^- transport by regulating the activity of NRT2, but they are not transport proteins themselves [28].

Pecan (*Carya illinoensis* (Wangenh.) K. Koch) belongs to the Juglandaceae family and is one of the world's famous nut tree species, indigenous to the United States and Mexico [29]. Pecans have a good development prospect in China because of the high content of various nutrients and the important economic value of the kernels [30]. However, as an important economic tree species introduced for many years in China, pecan still has the problem of insufficient yield, and low nitrogen use efficiency (NUE) is an important factor leading to the underproduction of pecan. The key way to improve NUE is to master the N absorption and utilization pattern of plants and the molecular regulation mechanism,

but there is no systematic and in-depth research on pecan in this subject. In this study, we determined the absorption characteristics of NH_4^+ and NO_3^- in different N forms. We identified 10 *AMT* and 69 *NRT* gene family members in pecan and classified them into different evolutionary subfamilies. Then, we analyzed their gene structure, replication events and expression patterns to explore their functions in varying N forms, and we provide a theoretical basis for improving the NUE of pecan.

2. Results

2.1. Identification and Sequence Analysis of *AMT* and *NRT* Gene Family Members in Pecan

A total of 11 *AMT* candidates were identified that contained *AMT* or *AMT*-like repeats, and 95 *NRT* candidates were identified that contained *NRT* or *NRT*-like repeats. After validation of *AMT* and *NRT* structural domains by Pfam and NCBI CD-search, 10 were identified as *AMT* gene family members, and 69 were identified as *NRT* gene family members. The *AMT* and *NRT* genes were renamed according to the *Arabidopsis* gene names as well as the NCBI blastp results for subsequent analysis. Table S3 provided details of *AMTs* and *NRTs*.

Sequence analysis of pecan *AMT* and *NRT* gene family members revealed that the number of exons in *AMTs* ranged from one to five, and in *NRTs* from two to nine. The CDS length of *AMTs* ranged from 471 to 1542 bp, and in *NRTs* from 1053 to 2826 bp. Most *AMTs* (9/10) and *NRTs* (56/69) were stable proteins with a low protein instability index (instability index < 40). GRAVY analysis showed that the hydration of *AMT* and *NRT* proteins in pecan was greater than 0, indicating that these proteins are hydrophobic. Subcellular localization predictions showed that most *AMTs* (9/10) localized to the cell membrane and most *NRTs* (64/69) localized to the vesicles.

2.2. Phylogenetic Analysis of *AMTs* and *NRTs* in Different Species

To decipher the evolutionary relationships and functional associations of pecan *AMTs* and *NRTs*, phylogenetic trees were constructed using pecan *AMT* and *NRT* proteins and other plants, respectively (Figures 1 and 2). According to the phylogenetic trees, all *AMT* proteins were divided into two distinct evolutionary branches: *AMT1* and *AMT2* with strong support (Bootstrap = 100%). The *AMT2* was further divided into three clusters: *AMT2a*, *AMT2b*, and *AMT2c*. *AMT1* was the largest branch and included 34 *AMTs* (four *CiAMTs*), *AMT2a* included two *CiAMTs*, *AMT2b* included three *CiAMTs*, and *AMT2c* had no pecan *AMT* gene family members.

All *NRT* proteins were divided into three main clades: *NRT1/PTR*, *NRT2*, and *NRT3* subfamily. The *NRT1* formed four subclasses, named *NRT1a*, *NRT1b*, *NRT1c*, and *NRT1d*, and included 62 *CiNRTs* and 52 *AtNRTs*. *NRT2* included five *CiNRTs* and seven *AtNRTs*, while *NRT3* included two *CiNRTs* and two *AtNRTs*. The evolutionary tree had 48 sister pairs, the majority of which were paralogous proteins, 38 pairs in total (21 pairs in pecan and 17 pairs in *Arabidopsis*), and 10 pairs of orthologous proteins. Only the *NRT3* subfamily had no orthologous proteins, while all other clades contained orthologous and paralogous proteins.

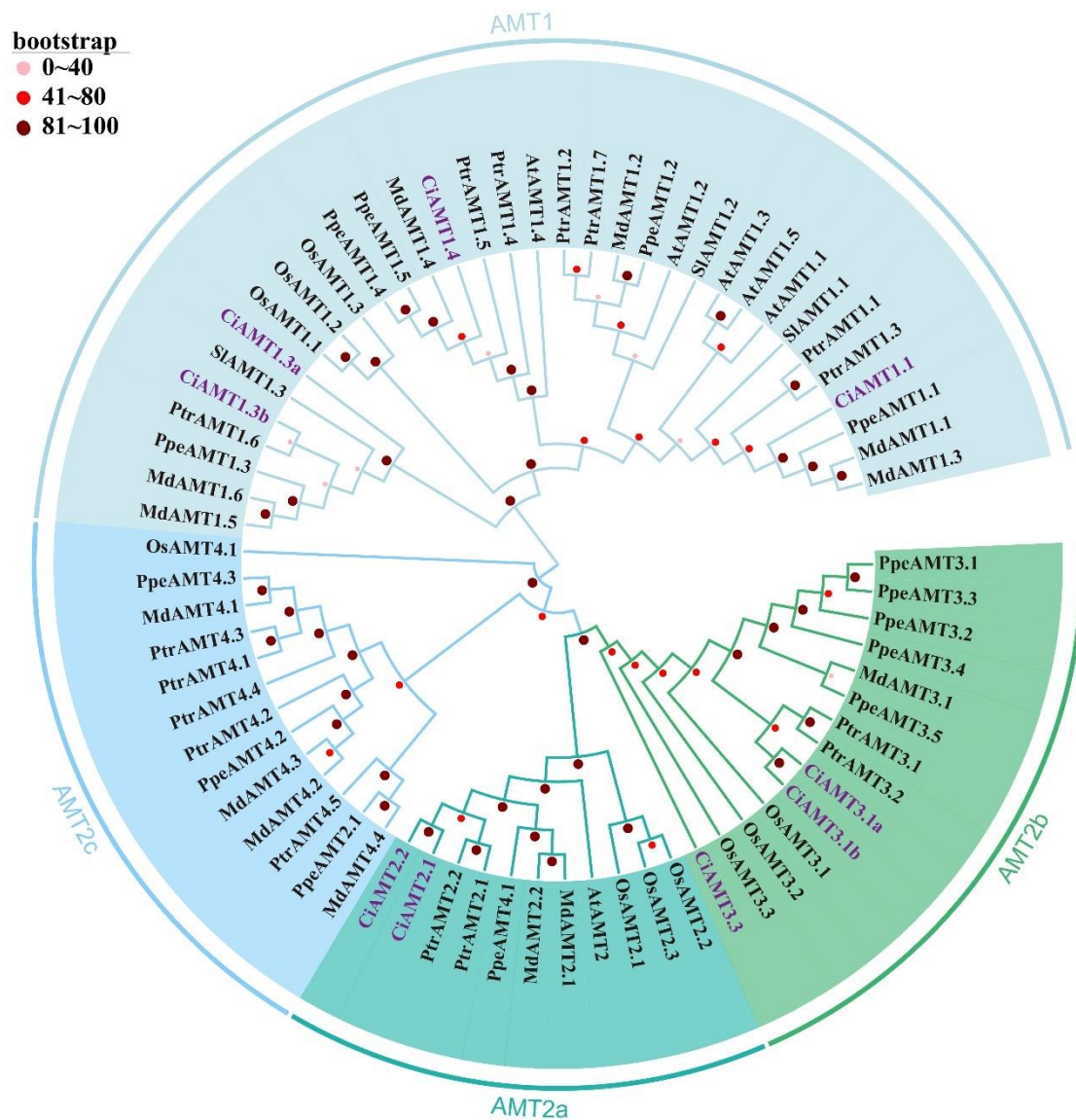


Figure 1. Phylogenetic analysis of AMT gene family in pecan (*Carya illinoensis*), poplar (*Populus trichocarpa*), apple (*Malus domestica*), peach (*Amygdalus persica* L.), tomato (*Lycopersicon esculentum* Miller), rice (*Oryza sativa* L.) and *Arabidopsis* (*Arabidopsis thaliana*). AMT proteins from seven species were divided into two subfamilies (AMT1 and AMT2). The AMT2 was further divided into three clusters (AMT2a, AMT2b, and AMT2c).

2.3. Phylogenetic Tree, Conserved Motif, Conserved Domain, and Gene Structural Analyses of CiAMTs and CiNRTs

To better understand the evolutionary relationships and functional associations of pecan AMT and NRT genes, we constructed unrooted phylogenetic trees with pecan AMT and NRT proteins, respectively (Figures 3A and 4A). According to MEME analysis, we found 10 motifs in most of the pecan AMT and NRT proteins (Figures 3B and 4B, Table S5). Motifs 1 to 7 were found in all AMT subfamilies, suggesting that these motifs may be characteristic motifs associated with members of the AMT gene family. Only 2–3 motifs in NRT2 were identical to the NRT1 subfamily, while NRT3 had no identical motifs to the NRT1 subfamily. We analyzed the structural domains of pecan AMT and NRT proteins using Pfam search and found that only one conserved Ammonium_trasp domain existed in all pecan AMT proteins, and they were all located at similar positions, while three conserved structural domains existed in pecan NRT proteins (Figures 3C and 4C, Table S4).

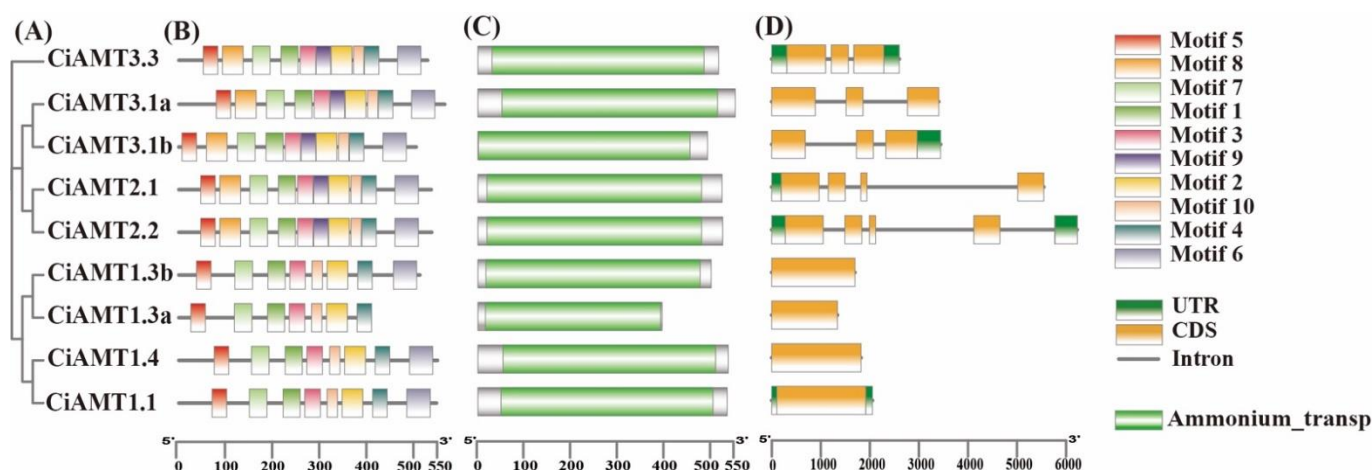


Figure 3. Phylogenetic analysis, conserved motif, conserved domain and gene structural of the *AMT* genes in pecan. Phylogenetic analysis of the *AMT* genes in pecan (A). The conserved motifs of the *AMT* genes in pecan (B). The conserved domain of the *AMT* genes in pecan (C). The gene structure of the *AMT* genes in pecan (D).

In addition, we analyzed the exons/introns of the pecan *AMT* and *NRT* genes to study the structural diversity. The results showed that the *AMT*1s contained no intron, and the *AMT*2s contained 2–4 introns (Figure 3D); the *NRT*1s had 2–9 introns, the *NRT*2s and *NRT*3s contained 1–2 introns (Figure 4D). In conclusion, the phylogenetic correlation between gene structure and prediction strongly supports a close evolutionary relationship between paired genes within the same subfamily.

2.4. Synteny Analysis of *CiAMTs* and *CiNRTs*

To determine the replication events of pecan *AMT* and *NRT* genes, we performed a synteny analysis of the pecan genome. The results showed that there were five duplicated gene pairs among the ten members of the pecan *AMT* gene family, two of which originated from tandem duplication and three from segmental duplication (Figure S1). There are 103 duplicated gene pairs among 69 members of the pecan *NRT* gene family, of which 9 originated from tandem duplication and 94 from segmental duplication. This suggested that fragment replication events played an important role in the expansion of the *AMT* and *NRT* gene families in pecan.

To examine the selection type of duplicate gene pairs in the pecan *AMT* and *NRT* gene families, the K_a/K_s ratios were analyzed for duplication events (Table S6). $K_a/K_s < 1$ means the gene is subjected to purifying selection, $K_a/K_s > 1$ means the gene underwent positive selection, and $K_a/K_s = 1$ means neutral evolution. The K_a/K_s values of all duplicate gene pairs were less than 1, indicating that the amplification of the pecan *AMT* and *NRT* genes was mainly influenced by purifying selection.

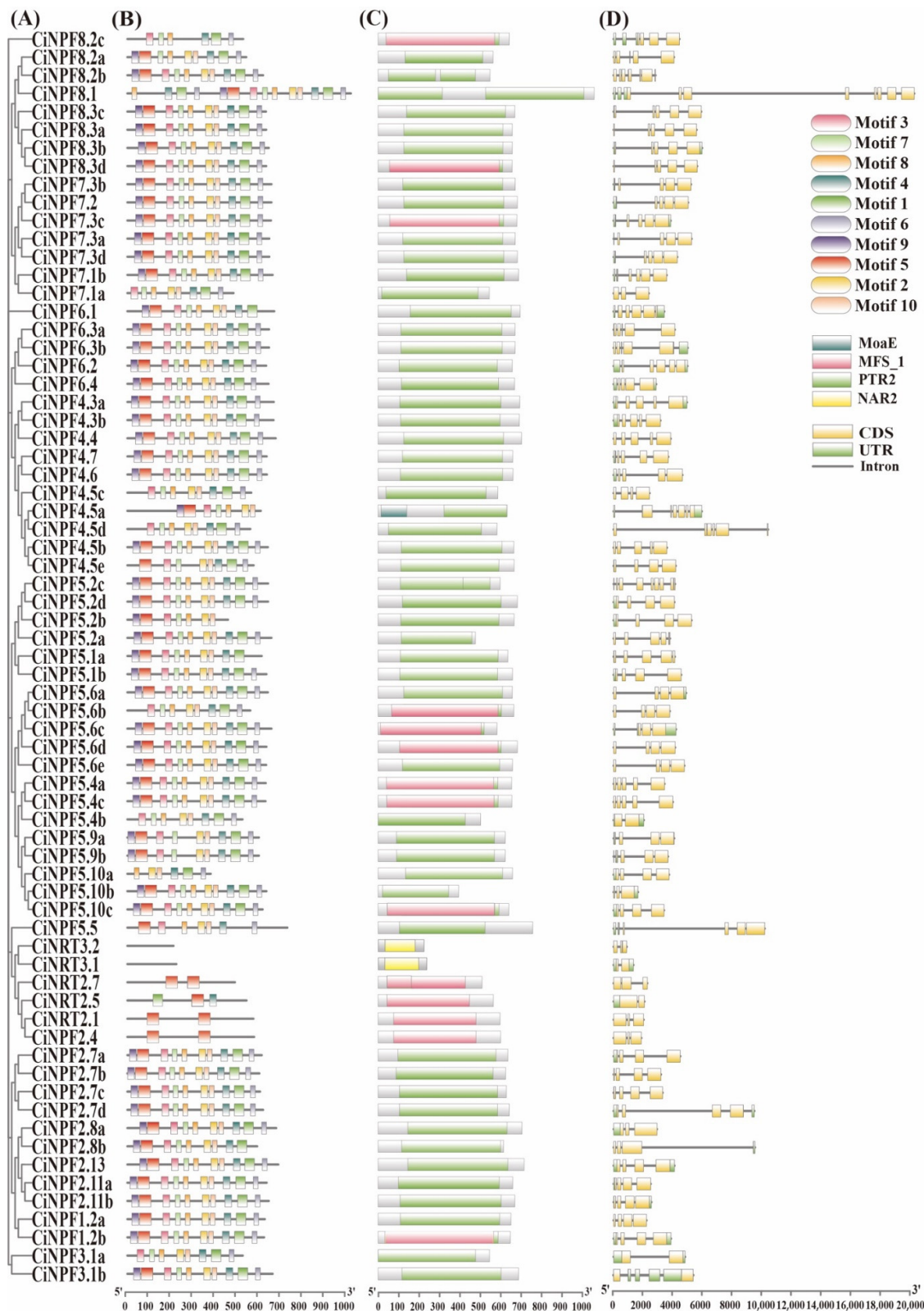


Figure 4. Phylogenetic analysis, conserved motif, conserved domain and gene structural of the *NRT* genes in pecan. Phylogenetic analysis of the *NRT* genes in pecan (A). The conserved motifs of the *NRT* genes in pecan (B). The conserved domains of the *NRT* genes in pecan (C). The gene structure of the *NRT* genes in pecan (D).

2.5. Effect of N Forms on Quantitative qRT-PCR Analysis of AMT and NRT Gene Expression Levels in Pecan

The results of qRT-PCR analysis of *CiAMTs* showed that the relative expression levels of *CiAMTs* were significantly affected by different N forms (Figure 5). The relative expression levels of almost all *CiAMTs* were higher in roots than in leaves, indicating that *CiAMTs* mainly worked in roots. In the roots, *CiAMT1.1* was significantly upregulated under T3 and T4 ($p < 0.05$), *CiAMT1.3a* was significantly upregulated only under T5 ($p < 0.05$), and *CiAMT1.3b*, *CiAMT1.4* and *CiAMT3.1a* were all significantly upregulated only under T4 ($p < 0.05$). *CiAMT2.1* was significantly upregulated under T1, T3, and T4 ($p < 0.05$), *CiAMT2.2* was significantly upregulated under T4 and T5 ($p < 0.05$), and *CiAMT3.1b* was significantly upregulated under T1, T2, and T3 ($p < 0.05$). The relative expression of *CiAMT3.3* was significantly upregulated under all N form treatments, with the most significant in T4 and T5 ($p < 0.05$). In leaves, all of them showed significant downregulated except *CiAMT2.1*, *CiAMT2.2*, *CiAMT3.1b*, and *CiAMT3.3*, which were significantly upregulated under individual treatments ($p < 0.05$).

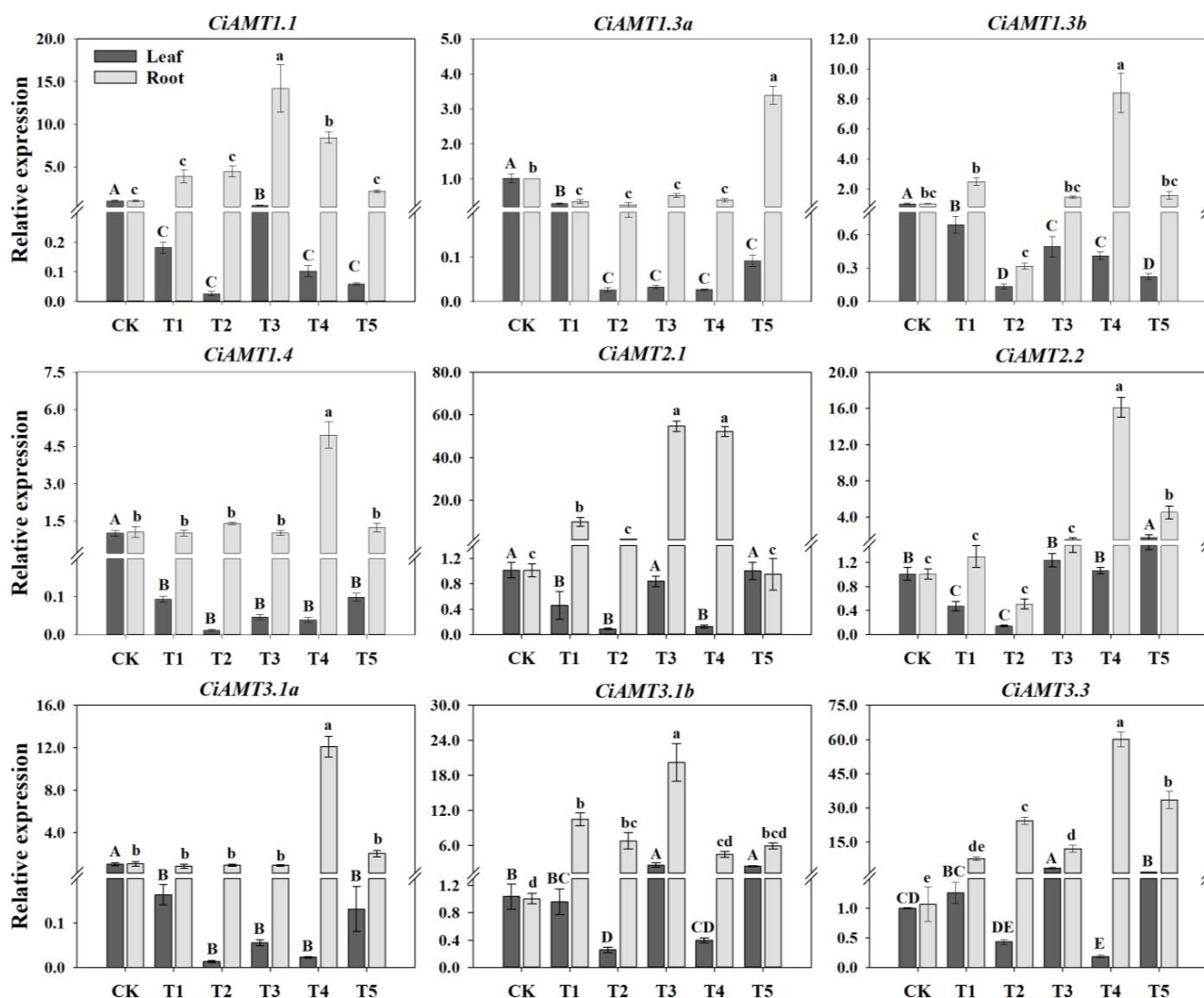


Figure 5. Relative expression of pecan *CiAMT* genes under varying $\text{NH}_4^+:\text{NO}_3^-$ ratios. The expression levels of *CiAMT* in pecan leaves and roots after varying $\text{NH}_4^+:\text{NO}_3^-$ ratio treatments were quantified by qRT-PCR, with *Actin* as the reference gene. Different capital letters indicate significant differences in leaves ($p < 0.05$), and different lowercase letters indicate significant differences in roots ($p < 0.05$).

Based on the results of previous studies [16], some members of the *Arabidopsis* and rice *NRT* gene families have been shown to be associated with NO_3^- uptake and transport. According to the phylogenetic tree, we selected 16 pecan *CiPawNRTs* corresponding to them and further analyzed them using qRT-PCR (Figure 6). The qRT-PCR results showed that *CiNRTs* showed different expression patterns in different N forms as well as in different pecan organs. Except for *CiNPF2.13*, *CiNPF4.6*, *CiNPF5.5*, *CiNPF6.3a*, *CiNPF6.4*, *CiNRT2.5*, and *CiNRT2.7*, which showed relative higher expression in leaves than in roots under most N form treatments, most of the other *CiNRTs* showed higher expression in roots than in leaves. In leaves, *CiNPF2.4* and *CiNPF2.13* under T1, *CiNPF5.5* under T1 and T4, *CiNPF7.2* under T3, *CiNRT2.7* under T1, and *CiNPF2.7b*, *CiNPF4.6*, *CiNPF5.9a*, *CiNPF5.10b* under T5 showed significantly upregulated expression ($p < 0.05$). In roots, *CiNPF1.2a* was significantly upregulated under T3 and T4 ($p < 0.05$), and *CiNPF2.7b* was significantly upregulated under T2 and T4 ($p < 0.05$). *CiNPF2.4* and *CiNPF2.11b* were significantly upregulated only with T3 ($p < 0.05$), while *CiNPF5.10b* was significantly upregulated only with T4 ($p < 0.05$). *CiNPF2.13*, *CiNPF6.4*, and *CiNRT2.7* were significantly downregulated under each N form treatment ($p < 0.05$), *CiNPF4.6* was significantly downregulated under T1, T2, and T5 ($p < 0.05$), while *CiNPF7.3a* was significantly downregulated under T1, T2, T3, and T5 ($p < 0.05$). *CiNPF5.5* was significantly upregulated under T2 as well as significantly downregulated under T3 ($p < 0.05$), *CiNPF6.2* was significantly upregulated under T2 as well as significantly downregulated under T1, T3, and T5 ($p < 0.05$), and *CiNPF6.3a* was significantly upregulated under T4 as well as significantly downregulated under T1, T2, and T3 ($p < 0.05$). *CiNPF7.2* was significantly upregulated under T3 and T4 and downregulated under T5 ($p < 0.05$). *CiNRT2.5* was significantly upregulated under T2 and T3 and downregulated under the other treatments ($p < 0.05$).

2.6. Effect of N Forms on NH_4^+ , NO_3^- and NO_2^- Concentration in Pecan

To further investigate the response mechanisms of pecan *AMT* and *NRT* genes to N forms, we measured the concentrations of NH_4^+ , NO_3^- , and NO_2^- in pecan under different N forms (Figure 7). The results showed that there was no significant difference in the NH_4^+ concentrations of pecan in all organs under different N forms. Except for the T5 treatment, NH_4^+ concentrations under all other treatments showed greater in roots than in leaves and stem ($p < 0.05$) and no significant difference between leaves and stems. The variability of NO_3^- concentrations in each organ of pecan varied among treatments, and T5 showed significantly greater than CK and T3 in leaves ($p < 0.05$), and no significant differences were found between T1, T2, T4, and other treatments. In the stems, no significant differences were found between treatments. In the roots, it showed that T4 was significantly greater than CK ($p < 0.05$), and T4 was not significantly different from the other treatments. Except for T3 and T5 treatment, the NO_3^- concentrations of pecan under all other treatments showed greater leaves than roots ($p < 0.05$) and no significant difference between stems, leaves, and roots. There was no significant difference in NO_2^- concentrations in all organs of pecan under different treatments, while the variability of NO_2^- concentrations in different organs under each treatment varied. CK, T1, and T5 showed no significant difference between stems and roots, and both of them were significantly greater than leaves ($p < 0.05$), T2 and T3 showed no significant difference between leaves and roots, and both of them were significantly greater than stems ($p < 0.05$), while T4 showed no significant variation in different organs.

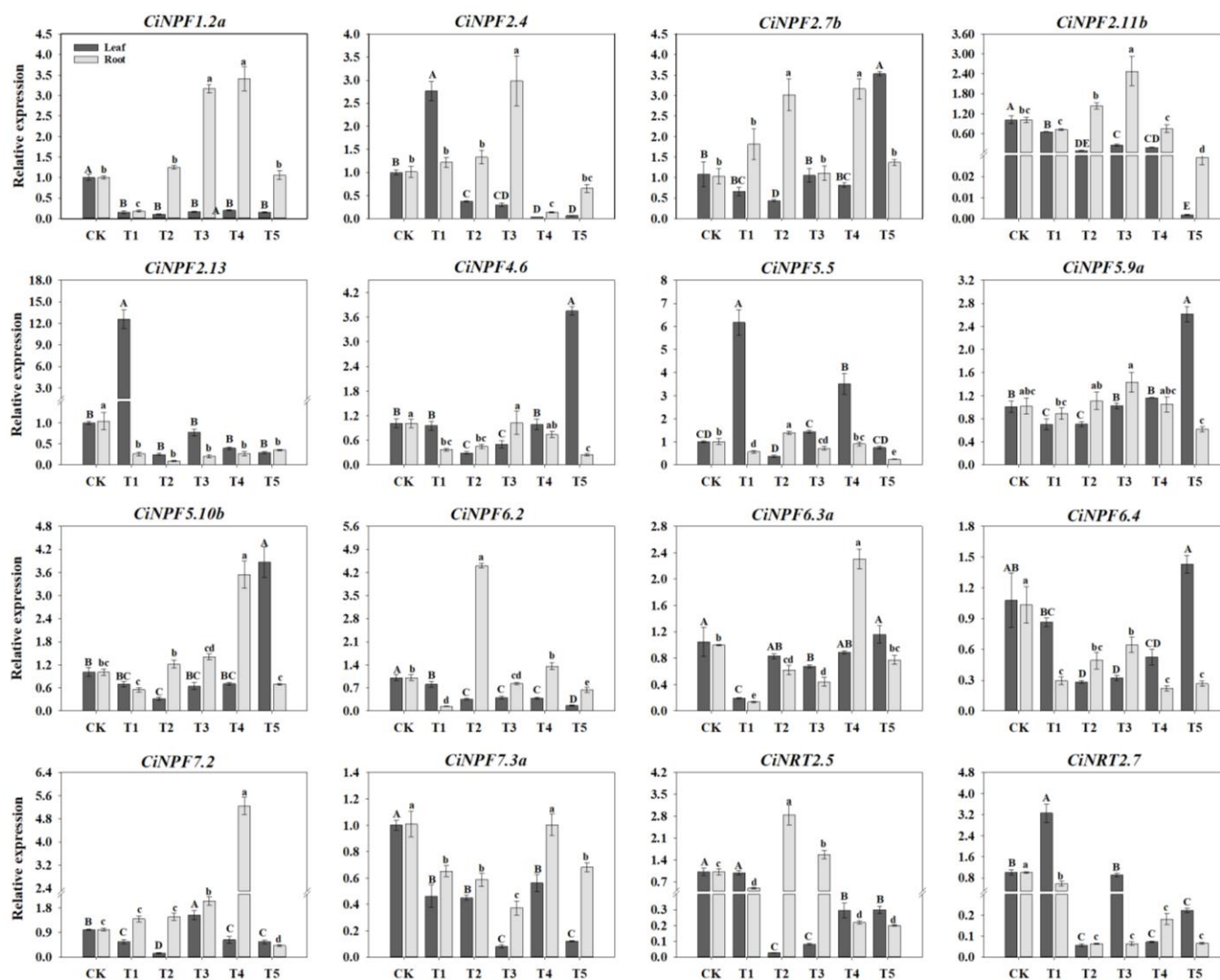


Figure 6. Relative expression of selected pecan *CiNRT* genes under varying $\text{NH}_4^+:\text{NO}_3^-$ ratios. The expression levels of selected *CiNRT* in pecan leaves and roots after varying $\text{NH}_4^+:\text{NO}_3^-$ ratio treatments were quantified by qRT-PCR, with *Actin* as the reference gene. Different capital letters indicate significant differences in leaves ($p < 0.05$), and different lowercase letters indicate significant differences in roots ($p < 0.05$).

At the mean level, pecan NH_4^+ concentrations were significantly greater in the T4 than in the other treatments ($p < 0.05$), with no significant differences between the other treatments. The pecan NO_3^- concentrations revealed no significant difference between T1, T4, and T5, and both of them were significantly greater than CK, T2, and T3 ($p < 0.05$). There was no significant difference between T2 and T1, T3 and T4, T2 was significantly greater than CK ($p < 0.05$), and no significant difference between CK and T3. The variability of pecan NO_2^- and NH_4^+ concentrations was consistent, suggesting that T4 was significantly greater than the other treatments ($p < 0.05$), with no significant differences between the other treatments.

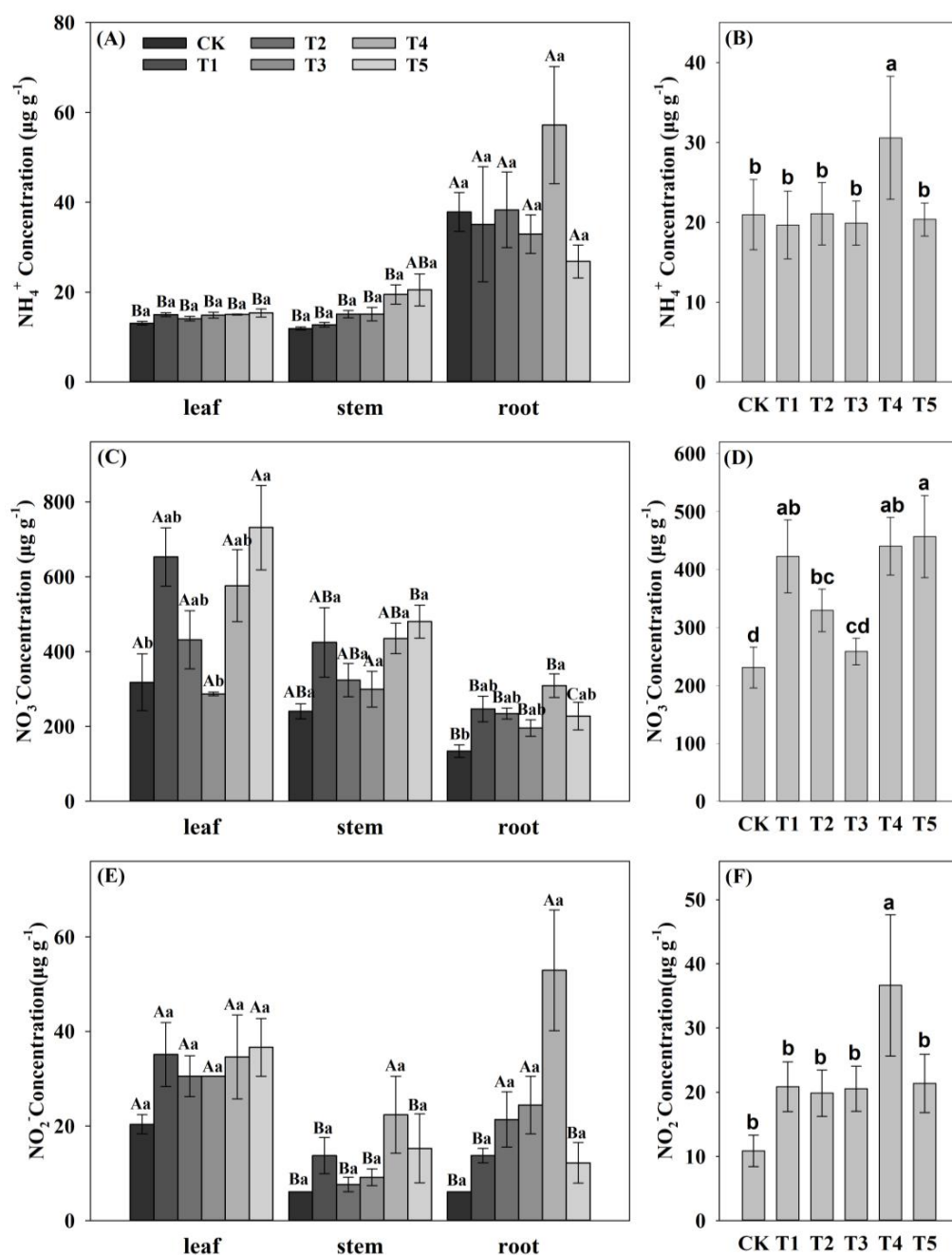


Figure 7. Differences of NH_4^+ , NO_3^- , and NO_2^- concentrations of pecan under varying $\text{NH}_4^+:\text{NO}_3^-$ ratios. Differences of NH_4^+ concentrations in pecan leaves, stems, and roots under varying $\text{NH}_4^+:\text{NO}_3^-$ ratios (A). The mean values of NH_4^+ concentrations in pecan leaves, stems, and roots under varying $\text{NH}_4^+:\text{NO}_3^-$ ratios (B). Differences of NO_3^- concentrations in pecan leaves, stems, and roots under varying $\text{NH}_4^+:\text{NO}_3^-$ ratios (C). The mean values of NO_3^- concentrations in pecan leaves, stems, and roots under varying $\text{NH}_4^+:\text{NO}_3^-$ ratios (D). Differences of NO_2^- concentrations in pecan leaves, stems, and roots under varying $\text{NH}_4^+:\text{NO}_3^-$ ratios (E). The mean values of NO_2^- concentrations in pecan leaves, stems, and roots under varying $\text{NH}_4^+:\text{NO}_3^-$ ratios (F). Upper capital letters indicate significant differences between organs ($p < 0.05$), and lowercase letters indicate significant differences between varying $\text{NH}_4^+:\text{NO}_3^-$ ratios ($p < 0.05$).

2.7. Effect of N Forms on the Uptake Kinetics of NH_4^+ and NO_3^- in Pecan

We also determined the kinetic properties of pecan NH_4^+ and NO_3^- uptake under different N forms (Figure 8). The results showed that the uptake rates of NH_4^+ and NO_3^-

under T2, T3, and T4 were still in a significant upward trend at the ion concentration of $2000 \mu\text{mol}\cdot\text{L}^{-1}$; the uptake rates of NH_4^+ and NO_3^- under CK, T1, and T5 leveled off at the medium ion concentration of $1000 \mu\text{mol}\cdot\text{L}^{-1}$.

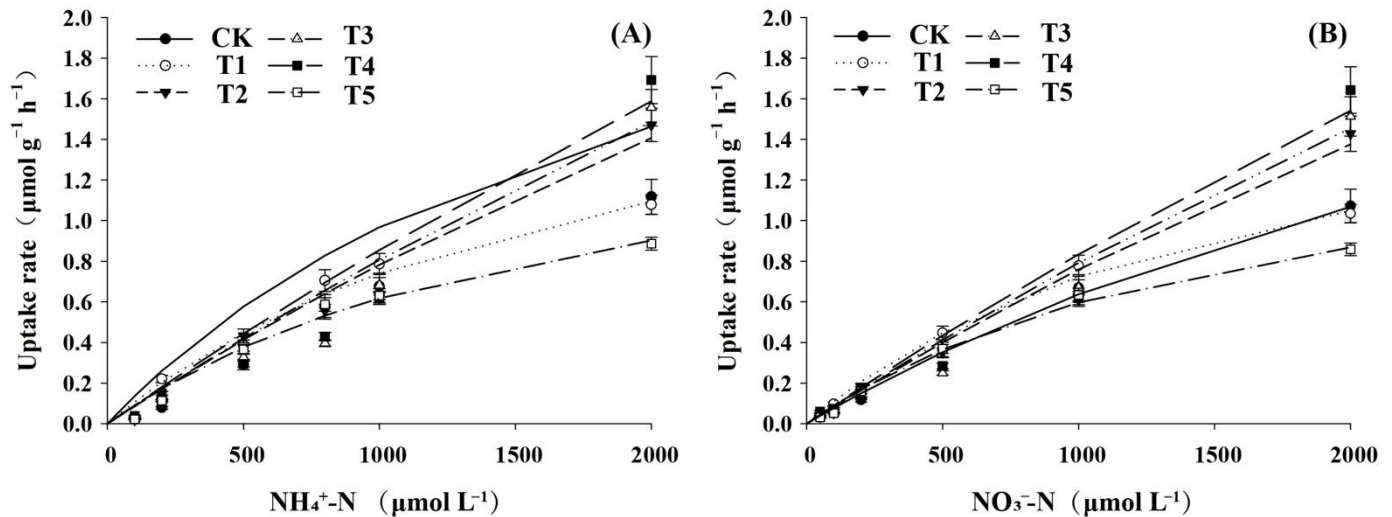


Figure 8. NH_4^+ and NO_3^- uptake rates of pecan under varying $\text{NH}_4^+:\text{NO}_3^-$ ratios. (A). NH_4^+ uptake rates of pecan under varying $\text{NH}_4^+:\text{NO}_3^-$ ratios (B). NO_3^- uptake rates of pecan under varying $\text{NH}_4^+:\text{NO}_3^-$ ratios.

The root uptake rates were processed data according to the Hofstee transformation equation to obtain the maximum uptake rate (V_m) and the Mee's constant (K_m) of pecan for different N forms with significant coefficients of determination R^2 (Table 1). Different N forms showed significant effects on V_{\max} and K_m of NH_4^+ and NO_3^- ($p < 0.05$), both showing $T4 > T3 > T2 > CK > T1 > T5$. This indicates that the involvement of a certain proportion of NH_4^+ accelerated the uptake of NH_4^+ and NO_3^- by pecans, but the affinity decreased, while NH_4^+ above a certain proportion decreased the uptake rate and increased the affinity. Except for the T1 treatment, the V_{\max}/K_m of NH_4^+ was greater than that of NO_3^- under all treatments, indicating that the rate of NH_4^+ uptake by pecan was greater than that of NO_3^- .

Table 1. N uptake kinetics of pecan roots under varying $\text{NH}_4^+:\text{NO}_3^-$ ratios. Lowercase letters indicate significant differences between varying $\text{NH}_4^+:\text{NO}_3^-$ ratios ($p < 0.05$).

Treatment	$\text{NH}_4^+\text{-N}$				$\text{NO}_3^-\text{-N}$			
	$V_{\max}/$ ($\mu\text{mol}\cdot\text{g}^{-1}\cdot\text{h}^{-1}$)	$K_m/$ ($\text{mmol}\cdot\text{L}^{-1}$)	V_{\max}/K_m	Goodness of Fit (R^2)	$V_{\max}/$ ($\mu\text{mol}\cdot\text{g}^{-1}\cdot\text{h}^{-1}$)	$K_m/$ ($\text{mmol}\cdot\text{L}^{-1}$)	V_{\max}/K_m	Goodness of Fit (R^2)
CK	3.00 ± 0.21 d	3.40 ± 0.07 d	0.89	0.975	3.30 ± 0.01 c	4.18 ± 0.47 c	0.81	0.996
T1	2.11 ± 0.00 d	1.85 ± 0.18 e	1.17	0.977	1.90 ± 0.02 d	1.62 ± 0.14 d	1.19	0.994
T2	6.96 ± 0.42 c	7.89 ± 0.21 c	0.88	0.966	7.33 ± 0.52 b	8.65 ± 0.18 b	0.85	0.979
T3	9.52 ± 0.93 b	10.80 ± 0.43 b	0.88	0.911	9.05 ± 0.78 a	10.43 ± 0.36 a	0.86	0.954
T4	11.13 ± 0.93 a	12.01 ± 0.39 a	0.92	0.942	10.10 ± 0.55 a	11.10 ± 0.35 a	0.91	0.976
T5	1.68 ± 0.02 d	1.72 ± 0.10 e	0.98	0.978	1.60 ± 0.01 d	1.68 ± 0.12 d	0.97	0.995

3. Discussion

3.1. Functional Differentiation of AMT and NRT Gene Family in Pecan Genome

The biological functions of *AMT* and *NRT* gene families in pecan are poorly understood. Therefore, we report for an earlier time identification of 10 *AMT* and 69 *NRT* gene family members from pecan, confirming that direct orthologs of *AMT* and *NRT* proteins should be highly conserved evolutionarily throughout the plant.

Studies on *Arabidopsis* *AMT* proteins have shown that *AtAMTs* had a prominent role in NH_4^+ assimilation at the cell membranes [10,11,31], and studies of flowering Chinese

cabbage (*Brassica campestris*) also indicated that BcAMT2 was located on the plasma membrane [32], which was consistent with the predicted results of subcellular localization in this study (Table S3), and this is the optimal cellular structure for maintaining stable NH_4^+ concentrations in plants. AtNPF5.11, AtNPF5.12, and AtNPF5.16 were identified to function in the process of NO_3^- from the vesicle to the cytoplasm, thereby regulating NO_3^- distribution between roots and shoots [33]. In contrast, the predicted subcellular localization of the pecan NRT genes in this study showed that most of the NRT1s were localized to the vacuoles (Table S3), suggesting that pecan NRT1s may mostly act in the transport of NO_3^- between the vacuoles and the cytoplasm. There were also some NRT1s localized on the cell membrane, while all NRT2s were all localized to the cell membrane, suggesting that this fraction of NRT proteins may mediate assimilation and efflux of NO_3^- in plants as well as inter-subcellular transport, which was consistent with the findings of cassava (*Manihot esculenta*) [34]. According to the predicted results of subcellular localization, the subcellular localization of all NRT3s differed significantly from NRT1 and NRT2 in pecan, with CiNRT3.1 localized to the nucleus and CiNRT3.2 localized on the cell membrane, cell wall, chloroplast, and vacuoles (Table S3), indicating that the pecan NRT3s had more complex structures and functions.

3.2. Effect of N Forms on the Absorption Characteristics of NH_4^+ and NO_3^- in Pecan

NH_4^+ and NO_3^- are the two main forms of N absorbed and utilized by plants, and previous studies have shown that a nutrient mixture of NH_4^+ and NO_3^- can improve crop yield and quality compared to a single source of N [35]. Therefore, understanding the best $\text{NH}_4^+:\text{NO}_3^-$ ratios provides the possibility to improve the N utilization efficiency of plants. We investigated the effect of varying $\text{NH}_4^+:\text{NO}_3^-$ ratios on the absorption and transport of N by measuring the concentrations of different N forms in the pecan organs (Figure 7).

This study showed that the concentrations of different N forms in pecan were tissue-specific. The NH_4^+ concentrations of pecan were significantly higher in roots than in leaves and stems, while NO_3^- and NO_2^- concentrations were significantly higher in leaves than in stems and roots, which was consistent with the finding that NH_4^+ was majorly assimilated in roots and NO_3^- was mostly translocated to leaves for storage or assimilation [36]. T4 significantly increased the total NH_4^+ concentrations of pecan, primarily in the roots, suggesting that T4 was more favorable to promote NH_4^+ absorbed by pecan roots, but had no effect on NH_4^+ transport between organs. All $\text{NH}_4^+:\text{NO}_3^-$ ratio treatments increased the total NO_3^- concentrations, primarily in the leaves, indicating that the feeding of NH_4^+ and NO_3^- mainly promoted the translocation of pecan NO_3^- from roots to leaves, and possibly the acclimation of NO_3^- in the leaves. Compared to T1, T3 reduced the total pecan NO_3^- concentrations, which was in agreement with the results of studies in pepper (*Capsicum annuum*) [37]. T4 significantly increased the total NO_2^- concentrations of pecan, indicating that T4 promoted the conversion of NO_3^- to NO_2^- .

Previous conclusions on the effects of the simultaneous presence of NH_4^+ and NO_3^- on each other's uptake were varied, with some suggesting that they have a facilitative or inhibitory effect [38,39], and that plant absorption of NH_4^+ and NO_3^- is limited by the maximum uptake threshold [40]. In this study, the uptake rates of NH_4^+ and NO_3^- gradually saturated with increasing substrate concentrations under a single N source, while they remained on an increasing trend under mixed N source treatments, with the T4 treatment being the most obvious, indicating that NH_4^+ and NO_3^- promoted each other's intake in this study, as evidenced by the magnitude of V_{max} values of pecan. However, single N source treatment increased the affinity of NH_4^+ and NO_3^- , and the combined application of NH_4^+ and NO_3^- decreased their affinity instead, which was generally consistent with the results of Kamminga-Van Wijk and Prins [41]. V_{max}/Km is also commonly used to indicate plant preference for NH_4^+ and NO_3^- uptake [42], suggesting that pecans may be more biased toward NH_4^+ absorption.

3.3. Effect of N Forms on the Expression of *CiAMTs* and *CiNRTs*

The ingestion and transport of NH_4^+ and NO_3^- in plants is majorly mediated by *AMT* and *NRT* gene family members. Therefore, we investigated the expression modes of these genes in varying organs and N forms to further understand the effect of N forms on N uptake and transport in pecan.

In the present study, the relative expression levels of almost all *CiAMTs* were higher in roots than in leaves, indicating that the addition of NH_4^+ and NO_3^- majorly stimulated the expression of *CiAMTs* in roots. Studies have shown that *AtAMT1.1*, *AtAMT1.2*, *AtAMT1.3*, and *AtAMT1.5* are the principal transporter proteins that take up high-affinity NH_4^+ into *Arabidopsis* roots, with *AtAMT1.1* and *AtAMT1.3* responsible for approximately two-thirds of the high-affinity NH_4^+ uptake capacity in the root; the *CiAMT1s* may have the same function [31,43]. The results of this study showed that all *CiAMT1s* were upregulated in roots of T4, except for *CiAMT1.3a*, which was upregulated in roots under T5, suggesting that T4 may have improved the absorption of high-affinity NH_4^+ by the pecan root. In this study, *CiAMT1s* were mostly upregulated in leaves under N lack, but numerous studies have shown that expression levels of *AMT1s* were upregulated in roots under N limited conditions [14,43,44]. This may be due to the variation caused by the longer duration of N deficiency in this study, or it is possible that the expression of *CiAMTs* in leaves was not only affected by N lack, but may also be involved in some other regulatory mechanisms [45]. Previous studies have shown that peach (*Prunus persica*) *PpeAMT3;4* was primarily expressed in roots [46], and the expression pattern of *CiAMT2s* was similar to that of *CiAMT1s*, being expressed mostly in roots and almost significantly upregulated at all timepoints under T4.

Studies on *Arabidopsis* suggested that *AtNPF6.3/AtNRT1.1* was not only an amphiphilic NO_3^- transport protein but might also act as a NO_3^- sensor under low NO_3^- conditions [47]. The expression level of *CiNPF6.3a* was significantly upregulated in roots under T4, suggesting that it may carry both translocation and signaling functions at this time. *AtNPF4.6/AtNRT1.2* was not only a low-affinity NO_3^- transporter protein that plays a role in NO_3^- influx [21], but also an abscisic acid (ABA) transporter protein that positively regulated the ABA response [48]. *CiNPF4.6* expression was significantly upregulated in roots under T3 and in leaves under T5, perhaps because *CiNPF4.6* worked primarily on NO_3^- influx under T3, while it worked mostly on ABA regulation under T5. *MtNPF6.8/MtNRT1.3* of *Medicago truncatula* was an amphiphilic NO_3^- transport protein and was upregulated by the absence of NO_3^- [49]. This was the same as the results of our study, where *CiNPF6.4/CiNRT1.3* expression was significantly upregulated in roots under CK and in leaves under T5. *AtNPF7.3/AtNRT1.5* mediated root-to-stem transport, and the same conclusion was found for *ZxNPF7.3/ZxNRT1.5* in the *Zygophyllum xanthoxylum*, which also contributed to the uptake of NO_3^- [50]. The expression levels of *CiNPF7.3a/CiNRT1.3a* were significantly upregulated in roots, leaves under CK, and roots under T4, indicating that both N scarcity and T4 may promote NO_3^- transport from roots to stems. Moreover, *AtNPF7.2/AtNRT1.8* was phylogenetically similar to *AtNPF7.3* [51], while *CiNPF7.2/CiNRT1.8* was also significantly upregulated in roots under T4 and may function similarly to *CiNPF7.3*. *NPF2.13/NRT1.7* and *NPF1.2/NRT1.11* were proven to be involved in the transfer and redistribution of NO_3^- from xylem or the NO_3^- containing tissues to the phloem [23], *CiNPF2.13* was largely induced by N limitation and T3, while *CiNPF1.2a* was mainly induced by N limitation, and T4. *NPF2.11/NRT1.10* was identified to be involved in thioglucoside transport [52], and *CiNPF2.11* expression was significantly upregulated under CK, suggesting that *CiNPF2.11* may resist N deficiency stress by regulating the concentrations of thioglucosides. *AtNRT2.5* was a plasma-membrane localized high-affinity NO_3^- transporter protein that mediated NO_3^- acquisition, and reactivation under N deficient conditions [27], and *CiNRT2.5* in this study exhibited the same expression pattern. The transcript levels of *NRT2.7* in *Fraxinus mandshurica* were both upregulated in leaves due to N limitation [53], whereas *CiNRT2.7* in this study was significantly expressed in roots under CK and in leaves under T1, which may be caused by species differences.

4. Materials and Methods

4.1. Plant Materials and Experimental Design

In the study, aeroponic cultivation trials were carried out in the greenhouse of the campus of Nanjing Forestry University from 18 April to 9 June 2021 and from 4 May to 21 June 2022. The plant materials and experimental design refer to Chen et al. [29]. In the case of the same N supply, the five ammonia-to-nitrate ratios ($\text{NH}_4^+:\text{NO}_3^-$) were 100:0, 75:25, 50:50, 25:75, and 0:100, corresponding to T1, T2, T3, T4, and T5, respectively. The nutrient solution without N was used as the control (CK), and each treatment was repeated 3 times, each with 6 seedlings. Regulation of the $\text{NH}_4^+:\text{NO}_3^-$ ratios for each treatment was achieved with specific source compounds (Table S1). Samples were taken after 45 days of treatment for further determination.

4.2. Identification of *AMT* and *NRT* Genes in Pecan

To identify the pecan *AMT* and *NRT* genes, we obtained all of the protein sequences of pecan from the Phytozome v13 database (https://phytozome-next.jgi.doe.gov/info/CillinoensisPawnee_v1_1 (accessed on 1 November 2021)). The hidden Markov model (HMM) profiles of the *AMT* domain (PF00909) and *NRT* domain (PF07690, PF00854, PF16974), downloaded from the Pfam database (<http://pfam.xfam.org/> (accessed on 1 February 2022)) [54], were used to identify the pecan *AMT* and *NRT* proteins by using HMM search through HMMER3.0 program (www.hmm.org (accessed on 1 February 2022)) with default parameters [55]. As multiple *AMT* and *NRT* proteins were corresponding to a specific gene in several cases, only one protein sequence corresponding to each gene was retained for further detailed analysis. The Pfam database was used to confirm the presence of these conserved domains of the screened genes. The biophysical properties such as amino acid length (AA), molecular weights (MWs), theoretical isoelectric points (pIs), and grand average of hydration (GRAVY) of pecan *AMT* and *NRT* proteins were estimated by ExpASy ProtParam server (<http://web.expasy.org/protparam> (accessed on 1 February 2022)) [56]. Transmembrane helices (TMHs) were determined using the TMHMM tools (<http://www.cbs.dtu.dk/services/TMHMM-2.0/> (accessed on 1 February 2022)), prediction of subcellular localization information for pecan *AMT* and *NRT* proteins using the Cell-PLoc 2.0 software (<http://www.csbio.sjtu.edu.cn/bioinf/Cell-PLoc-2/> (accessed on 1 February 2022)) [57].

4.3. Phylogenetic Analysis

The *Arabidopsis* *AMT* and *NRT* protein sequences were downloaded from the TAIR database (<https://www.arabidopsis.org/> (accessed on 1 November 2021)) [58]. The poplar, apple, pear, tomato, and rice *AMT* protein sequences were downloaded from the Phytozome database. Phylogenetic trees were constructed by MEGA 7.0 with the following settings: the neighbor-joining (NJ) method, 1000 bootstrap replicates, the Jones–Taylor–Thornton (JTT) model, and pairwise deletion [59]. The evolutionary tree was visualized using the online tool Evolview (<http://evolgenius.info/> (accessed on 1 March 2022)) [60]. Because *CiAMT3.1c* is a partial sequence, it was not included in the phylogenetic tree.

4.4. Analysis of Gene Structure, Conservative Motifs, and Domains

The pecan genome sequence files and the General Feature Format (GFF) annotation files were downloaded from the Phytozome database. We used the online MEME tool (<http://MEME-suite.org/> (accessed on 1 April 2022)) for topic prediction, keeping the maximum number of topics at 10 [61]. TBtools visualizes *AMT* and *NRT* gene structures, conservative motifs, and domains [62].

4.5. Synteny Analysis

For detecting syntenic blocks, the whole genome sequence file and the GFF annotation file of pecan were used to identify all duplication events in the pecan genome using

MCSanX software [63]. Then, the *AMT* and *NRT* gene families were analyzed for synteny and visualized using TBtools.

4.6. Estimation of the *Ka/Ks* Values

Multiple sequence alignment of full-length coding sequences (CDS) in the *AMT* and *NRT* gene families in pecan was performed using MEGA 7 software and further used to calculate nonsynonymous (*Ka*) and synonymous (*Ks*), and the *Ka/Ks* ratios. *Ks* values were commonly used to determine the time since gene duplication, and the selection pressure of duplication event was determined by the *Ka/Ks* ratio.

4.7. *Cis-Regulatory Elements Analysis*

To investigate potential *cis*-regulatory elements in the promoters of the pecan *AMT* and *NRT* genes, a 1000 bp region upstream of the *AMT* and *NRT* genes was retrieved from the pecan genome sequences. Then, the *cis*-regulatory elements were predicted using PlantCARE software (<http://bioinformatics.psb.ugent.be/webtools/plantcare/html/> (accessed on 1 April 2022)) [64] and screened and visualized by TBtools software (Figures S2 and S3).

4.8. Protein–Protein Interaction Network Prediction

Protein–protein interaction networks of *AMT* and *NRT* gene families were analyzed by String (<https://string-db.org/> (accessed on 1 April 2022)) (Figure S4) [65].

4.9. RNA Collection and qRT-PCR Expression Analysis

According to the manufacturer's protocol, the total RNA was extracted from the leaves and roots of pecan using a Universal Plant Total RNA Extraction Kit (Bioteke, Beijing, China) and stored at $-80\text{ }^{\circ}\text{C}$ until further use. The purity and integrity of the isolated total RNA were analyzed by agarose gel electrophoresis and Nanodrop 2000 spectrophotometer (Thermo Scientific, Wilmington, NC, USA). First-strand cDNA was synthesized using a cDNA Synthesis Kit (HiScript[®]RIII RT SuperMix for qPCR +gDNA wiper, Vazyme, Nanjing, China). The qRT-PCR was performed on a 7500 Real-Time PCR system (Applied Biosystems[™], Foster City, CA, USA) using a Taq Pro Universal SYBR qPCR Master Mix (Vazyme, Nanjing, China). The specific primers were synthesized by Tsingke Biotechnology Ltd. (Nanjing, China), and the details of the primers were provided in Supplementary Table S2. The PCR parameters applied here were as follows: $95\text{ }^{\circ}\text{C}$ for 30 s, followed by 40 cycles of 5 s at $95\text{ }^{\circ}\text{C}$ and 30 s at $60\text{ }^{\circ}\text{C}$. The *Actin* gene was used as an internal reference gene [66], and the relative expression levels of pecan *AMT* and *NRT* genes were determined using the $2^{-\Delta\Delta\text{Ct}}$ method [67]. Values represent mean calculated from three biological replicates and three technological repeats.

4.10. Measurement of NH_4^+ , NO_3^- and NO_2^- Concentration in Pecan

The NH_4^+ concentrations of pecan roots, stems and leaves were determined according to the Berthelot reaction [68]. NO_3^- concentrations were determined according to the method suggested by Patterson et al. [69]. The NO_2^- concentrations were determined by the method of Ogawa et al. [70].

4.11. Kinetic Characterization of NH_4^+ and NO_3^- Uptake in Pecan

The kinetic characteristics of NH_4^+ and NO_3^- uptake in pecan seedlings were determined by the conventional depletion method, the ion concentrations in the solutions to be measured were determined after preparing different concentrations of NH_4^+ and NO_3^- for 24 h incubation of the plants, the net rate of ion uptake per unit fresh root per unit time was calculated, and the kinetic parameters of uptake were mathematically derived. The concentration of NH_4^+ and NO_3^- was determined by referring to 2.10.

4.12. Data Analysis

Before analysis of variance (ANOVA), data were checked for normality and homogeneity of variances. One-way ANOVA was performed to test the effects of different N forms on NH_4^+ , NO_3^- , NO_2^- concentrations, absorption kinetic characteristics and relative gene expression of pecan seedlings. Differences were considered significant at $p < 0.05$.

The kinetic parameters of NH_4^+ and NO_3^- uptake were calculated using the Hofstee transformation of the Michaelis–Menten kinetic equation: $V = C \times V_{\text{max}} / (K_m + C)$, C represents the ion concentration, V indicates the net ion uptake rate, V_m indicates the maximum uptake rate, and the K_m value represents the root uptake site for ion affinity. Non-linear regression fitting and graphing were performed using SPSS to obtain the V_{max} and K_m . The α value represents the competitive ability of the plant root system for nutrient uptake, $\alpha = V_{\text{max}} / K_m$.

All statistical analyses were performed with SPSS 23.0 software (Version 23.0, Chicago, IL, USA). All charts were drawn with Excel (Version 2019, Redmond, WA, USA) and SigmaPlot (Version 14.0, Barcelona, Spain).

5. Conclusions

We identified 10 *AMT* and 69 *NRT* genes in the pecan genome, and the analysis showed that the biophysical properties, gene structure, and expression levels of *CiAMTs* and *CiNRTs* were strongly associated with pecan NH_4^+ and NO_3^- uptake. Combining the effects of different N form treatments on the expression levels of *CiAMTs* and *CiNRTs*, the N concentrations of pecan, and the uptake rate of NH_4^+ and NO_3^- , we concluded that pecan preferred NH_4^+ and that the $\text{NH}_4^+ / \text{NO}_3^-$ ratio of 75:25 was more favorable to improve the N uptake capacity of pecan seedlings. This study provides a basis for further identification of the functions of *AMT* and *NRT* genes in N uptake and transport of pecan, and it provides a theoretical basis for the application of an optimal proportion of N fertilizer to improve NUE, thereby increasing pecan yield and promoting pecan industrialization.

Supplementary Materials: The following supporting information can be downloaded at: <https://www.mdpi.com/article/10.3390/ijms232113314/s1>.

Author Contributions: F.P. conceived and designed the study. M.C. collected experimental data, analyzed, and wrote the manuscript. M.C. and J.L. participated in the collection of samples. M.C. and J.X. performed the experiments. P.T. and K.Z. provided help in data analysis and in improving the manuscript. All authors have read and agreed to the published version of the manuscript.

Funding: This research was funded by a grant from the National Key R&D Program of China (2021YFD1000403) and the Central Financial Forestry Science and Technology Extension Demonstration Funds Program (Su (2022) TG04).

Conflicts of Interest: The authors declare no conflict of interest.

References

1. Nacry, P.; Bouguyon, E.; Gojon, A. Nitrogen Acquisition by Roots: Physiological and Developmental Mechanisms Ensuring Plant Adaptation to a Fluctuating Resource. *Plant Soil* **2013**, *370*, 1–29. [[CrossRef](#)]
2. Van Tichelen, K.K.; Colpaert, J.V. Kinetics of Phosphate Absorption by Mycorrhizal and Non-Mycorrhizal Scots Pine Seedlings. *Physiol. Plant.* **2000**, *110*, 96–103. [[CrossRef](#)]
3. Wang, L.; Macko, S.A. Constrained Preferences in Nitrogen Uptake across Plant Species and Environments: Plant Nitrogen Preference. *Plant Cell Environ.* **2011**, *34*, 525–534. [[CrossRef](#)] [[PubMed](#)]
4. Gazzarrini, S.; Lejay, L.; Gojon, A.; Ninnemann, O.; Frommer, W.B.; von Wirén, N. Three Functional Transporters for Constitutive, Diurnally Regulated, and Starvation-Induced Uptake of Ammonium into *Arabidopsis* Roots. *Plant Cell* **1999**, *11*, 937–948. [[CrossRef](#)]
5. Bai, H.; Euring, D.; Volmer, K.; Janz, D.; Polle, A. The Nitrate Transporter (NRT) Gene Family in Poplar. *PLoS ONE* **2013**, *8*, e72126. [[CrossRef](#)] [[PubMed](#)]
6. Ariz, I.; Boeckstaens, M.; Gouveia, C.; Martins, A.P.; Sanz-Luque, E.; Fernández, E.; Soveral, G.; von Wirén, N.; Marini, A.M.; Aparicio-Tejo, P.M.; et al. Nitrogen Isotope Signature Evidences Ammonium Deprotonation as a Common Transport Mechanism for the AMT-Mep-Rh Protein Superfamily. *Sci. Adv.* **2018**, *4*, eaar3599. [[CrossRef](#)]

7. Huang, L.; Li, J.; Zhang, B.; Hao, Y.; Ma, F. Genome-Wide Identification and Expression Analysis of *AMT* Gene Family in Apple (*Malus domestica* Borkh.). *Horticulturae* **2022**, *8*, 457. [[CrossRef](#)]
8. Song, S.; He, Z.; Huang, X.; Zhong, L.; Liu, H.; Sun, G.; Chen, R. Cloning and Characterization of the Ammonium Transporter Genes *BaAMT_{1;1}* and *BaAMT_{1;3}* from Chinese Kale. *Hortic. Environ. Biotechnol.* **2017**, *58*, 178–186. [[CrossRef](#)]
9. Castro-Rodríguez, V.; Assaf-Casals, I.; Pérez-Tienda, J.; Fan, X.; Avila, C.; Miller, A.; Cánovas, F.M. Deciphering the Molecular Basis of Ammonium Uptake and Transport in Maritime Pine. *Plant Cell Environ.* **2016**, *39*, 1669–1682. [[CrossRef](#)]
10. Giehl, R.F.H.; Laginha, A.M.; Duan, F.; Rentsch, D.; Yuan, L.; von Wirén, N. A Critical Role of *AMT2;1* in Root-To-Shoot Translocation of Ammonium in *Arabidopsis*. *Mol. Plant* **2017**, *10*, 1449–1460. [[CrossRef](#)]
11. Shelden, M.C.; Dong, B.; de Bruxelles, G.L.; Trevaskis, B.; Whelan, J.; Ryan, P.R.; Howitt, S.M.; Udvardi, M.K. *Arabidopsis* Ammonium Transporters, *AtAMT1;1* and *AtAMT1;2*, Have Different Biochemical Properties and Functional Roles. *Plant Soil* **2001**, *231*, 151–160. [[CrossRef](#)]
12. Yuan, L.; Graff, L.; Loqué, D.; Kojima, S.; Tsuchiya, Y.N.; Takahashi, H.; von Wirén, N. *AtAMT1;4*, a Pollen-Specific High-Affinity Ammonium Transporter of the Plasma Membrane in *Arabidopsis*. *Plant Cell Physiol.* **2009**, *50*, 13–25. [[CrossRef](#)] [[PubMed](#)]
13. Ludewig, U.; Neuhäuser, B.; Dynowski, M. Molecular Mechanisms of Ammonium Transport and Accumulation in Plants. *FEBS Lett.* **2007**, *581*, 2301–2308. [[CrossRef](#)]
14. Couturier, J.; Montanini, B.; Martin, F.; Brun, A.; Blaudez, D.; Chalot, M. The Expanded Family of Ammonium Transporters in the Perennial Poplar Plant. *New Phytol.* **2007**, *174*, 137–150. [[CrossRef](#)] [[PubMed](#)]
15. Tavares, O.C.H.; Santos, L.A.; Ferreira, L.M.; Sperandio, M.V.L.; da Rocha, J.G.; García, A.C.; Dobbss, L.B.; Berbara, R.L.L.; de Souza, S.R.; Fernandes, M.S. Humic Acid Differentially Improves Nitrate Kinetics under Low- and High-Affinity Systems and Alters the Expression of Plasma Membrane H⁺-ATPases and Nitrate Transporters in Rice. *Ann. Appl. Biol.* **2017**, *170*, 89–103. [[CrossRef](#)]
16. Kant, S. Understanding Nitrate Uptake, Signaling and Remobilisation for Improving Plant Nitrogen Use Efficiency. *Semin. Cell Dev. Biol.* **2018**, *74*, 89–96. [[CrossRef](#)]
17. Wang, Y.-Y.; Hsu, P.-K.; Tsay, Y.-F. Uptake, Allocation and Signaling of Nitrate. *Trends Plant Sci.* **2012**, *17*, 458–467. [[CrossRef](#)]
18. Wang, Y.-Y.; Cheng, Y.-H.; Chen, K.-E.; Tsay, Y.-F. Nitrate Transport, Signaling, and Use Efficiency. *Annu. Rev. Plant Biol.* **2018**, *69*, 85–122. [[CrossRef](#)]
19. Liu, K.H.; Huang, C.Y.; Tsay, Y.F. *CHL1* Is a Dual-Affinity Nitrate Transporter of *Arabidopsis* Involved in Multiple Phases of Nitrate Uptake. *Plant Cell* **1999**, *11*, 865–874. [[CrossRef](#)]
20. Tsay, Y.-F.; Chiu, C.-C.; Tsai, C.-B.; Ho, C.-H.; Hsu, P.-K. Nitrate Transporters and Peptide Transporters. *FEBS Lett.* **2007**, *581*, 2290–2300. [[CrossRef](#)]
21. Huang, N.-C.; Liu, K.-H.; Lo, H.-J.; Tsay, Y.-F. Cloning and Functional Characterization of an *Arabidopsis* Nitrate Transporter Gene That Encodes a Constitutive Component of Low-Affinity Uptake. *Plant Cell* **1999**, *11*, 1381–1392. [[CrossRef](#)] [[PubMed](#)]
22. Segonzac, C.; Boyer, J.-C.; Ipotesi, E.; Szponarski, W.; Tillard, P.; Touraine, B.; Sommerer, N.; Rossignol, M.; Gibrat, R. Nitrate Efflux at the Root Plasma Membrane: Identification of an *Arabidopsis* Excretion Transporter. *Plant Cell* **2007**, *19*, 3760–3777. [[CrossRef](#)] [[PubMed](#)]
23. Iqbal, A.; Qiang, D.; Alamzeb, M.; Xiangru, W.; Huiping, G.; Hengheng, Z.; Nianchang, P.; Xiling, Z.; Meizhen, S. Untangling the Molecular Mechanisms and Functions of Nitrate to Improve Nitrogen Use Efficiency. *J. Sci. Food Agric.* **2020**, *100*, 904–914. [[CrossRef](#)]
24. Krapp, A.; David, L.C.; Chardin, C.; Girin, T.; Marmagne, A.; Leprince, A.-S.; Chaillou, S.; Ferrario-Méry, S.; Meyer, C.; Daniel-Vedele, F. Nitrate Transport and Signalling in *Arabidopsis*. *J. Exp. Bot.* **2014**, *65*, 789–798. [[CrossRef](#)]
25. Ma, H.; Zhao, J.; Feng, S.; Qiao, K.; Gong, S.; Wang, J.; Zhou, A. Heterologous Expression of Nitrate Assimilation Related-Protein *DsNAR2.1/NRT3.1* Affects Uptake of Nitrate and Ammonium in Nitrogen-Starved *Arabidopsis*. *Int. J. Mol. Sci.* **2020**, *21*, 4027. [[CrossRef](#)] [[PubMed](#)]
26. Li, W.; Wang, Y.; Okamoto, M.; Crawford, N.M.; Siddiqi, M.Y.; Glass, A.D.M. Dissection of the *AtNRT2.1:AtNRT2.2* Inducible High-Affinity Nitrate Transporter Gene Cluster. *Plant Physiol.* **2007**, *143*, 425–433. [[CrossRef](#)]
27. Lezhneva, L.; Kiba, T.; Feria-Bourrellier, A.-B.; Lafouge, F.; Boutet-Mercey, S.; Zoufan, P.; Sakakibara, H.; Daniel-Vedele, F.; Krapp, A. The *Arabidopsis* Nitrate Transporter *NRT2.5* Plays a Role in Nitrate Acquisition and Remobilization in Nitrogen-Starved Plants. *Plant J.* **2014**, *80*, 230–241. [[CrossRef](#)]
28. Kotur, Z.; Mackenzie, N.; Ramesh, S.; Tyerman, S.D.; Kaiser, B.N.; Glass, A.D.M. Nitrate Transport Capacity of the *Arabidopsis* Thaliana *NRT2* Family Members and Their Interactions with *AtNAR2.1*. *New Phytol.* **2012**, *194*, 724–731. [[CrossRef](#)]
29. Chen, M.; Zhu, K.; Tan, P.; Liu, J.; Xie, J.; Yao, X.; Chu, G.; Peng, F. Ammonia–Nitrate Mixture Dominated by NH₄⁺-N Promoted Growth, Photosynthesis and Nutrient Accumulation in Pecan (*Carya illinoensis*). *Forests* **2021**, *12*, 1808. [[CrossRef](#)]
30. Zhu, K.; Fan, P.; Liu, H.; Tan, P.; Ma, W.; Mo, Z.; Zhao, J.; Chu, G.; Peng, F. Insight into the CBL and CIPK Gene Families in Pecan (*Carya illinoensis*): Identification, Evolution and Expression Patterns in Drought Response. *BMC Plant Biol.* **2022**, *22*, 221. [[CrossRef](#)]
31. Yuan, L.; Loqué, D.; Kojima, S.; Rauch, S.; Ishiyama, K.; Inoue, E.; Takahashi, H.; von Wirén, N. The Organization of High-Affinity Ammonium Uptake in *Arabidopsis* Roots Depends on the Spatial Arrangement and Biochemical Properties of *AMT1*-Type Transporters. *Plant Cell* **2007**, *19*, 2636–2652. [[CrossRef](#)] [[PubMed](#)]

32. Zhu, Y.; Hao, Y.; Liu, H.; Sun, G.; Chen, R.; Song, S. Identification and Characterization of Two Ammonium Transporter Genes in Flowering Chinese Cabbage (*Brassica campestris*). *Plant Biotechnol.* **2018**, *35*, 59–70. [[CrossRef](#)] [[PubMed](#)]
33. He, Y.-N.; Peng, J.-S.; Cai, Y.; Liu, D.-F.; Guan, Y.; Yi, H.-Y.; Gong, J.-M. Tonoplast-Localized Nitrate Uptake Transporters Involved in Vacuolar Nitrate Efflux and Reallocation in *Arabidopsis*. *Sci. Rep.* **2017**, *7*, 6417. [[CrossRef](#)] [[PubMed](#)]
34. You, L.; Wang, Y.; Zhang, T.; Zhu, Y.; Ren, N.; Jiang, X.; Zhou, Y. Genome-Wide Identification of Nitrate Transporter 2 (NRT2) Gene Family and Functional Analysis of *MeNRT2.2* in Cassava (*Manihot esculenta* Crantz). *Gene* **2022**, *809*, 146038. [[CrossRef](#)]
35. Zhu, Y.; Qi, B.; Hao, Y.; Liu, H.; Sun, G.; Chen, R.; Song, S. Appropriate $\text{NH}_4^+/\text{NO}_3^-$ Ratio Triggers Plant Growth and Nutrient Uptake of Flowering Chinese Cabbage by Optimizing the PH Value of Nutrient Solution. *Front. Plant Sci.* **2021**, *12*, 724–739. [[CrossRef](#)]
36. Oh, K.; Kato, T.; Xu, H.L. Transport of Nitrogen Assimilation in Xylem Vessels of Green Tea Plants Fed with NH_4^+ -N and NO_3^- -N. *Pedosphere* **2008**, *18*, 222–226. [[CrossRef](#)]
37. Zhang, J.; Lv, J.; Dawuda, M.M.; Xie, J.; Yu, J.; Li, J.; Zhang, X.; Tang, C.; Wang, C.; Gan, Y. Appropriate Ammonium-Nitrate Ratio Improves Nutrient Accumulation and Fruit Quality in Pepper (*Capsicum annum* L.). *Agronomy* **2019**, *9*, 683. [[CrossRef](#)]
38. Ruan, L.; Wei, K.; Wang, L.; Cheng, H.; Zhang, F.; Wu, L.; Bai, P.; Zhang, C. Characteristics of NH_4^+ and NO_3^- Fluxes in Tea (*Camellia Sinensis*) Roots Measured by Scanning Ion-Selective Electrode Technique. *Sci. Rep.* **2016**, *6*, 38370. [[CrossRef](#)]
39. Wu, S.; Hua, J.; Lu, Y.; Zhang, R.; Yin, Y. Characteristics of NH_4^+ and NO_3^- Fluxes in Taxodium Roots under Different Nitrogen Treatments. *Plants* **2022**, *11*, 894. [[CrossRef](#)]
40. Tang, Y.; Gao, F.; Yu, Q.; Guo, S.; Li, F. The Uptake Kinetics of NH_4^+ and NO_3^- by Lettuce Seedlings under Hypobaric and Hypoxic Conditions. *Sci. Hortic.* **2015**, *197*, 236–243. [[CrossRef](#)]
41. Kamminga-Van Wijk, C.; Prins, H.B.A. The Kinetics of NH_4^+ and NO_3^- Uptake by Douglas Fir from Single N-Solutions and from Solutions Containing Both NH_4^+ and NO_3^- . *Plant Soil* **1993**, *151*, 91. [[CrossRef](#)]
42. Nishikawa, T.; Tarutani, K.; Yamamoto, T. Nitrate and Phosphate Uptake Kinetics of the Harmful Diatom *Coscinodiscus Wailesii*, a *Causative organism* in the Bleaching of Aquacultured *Porphyra thalli*. *Harmful Algae* **2010**, *9*, 563–567. [[CrossRef](#)]
43. Loqué, D.; Yuan, L.; Kojima, S.; Gojon, A.; Wirth, J.; Gazzarrini, S.; Ishiyama, K.; Takahashi, H.; Von Wirén, N. Additive Contribution of AMT1;1 and AMT1;3 to High-Affinity Ammonium Uptake across the Plasma Membrane of Nitrogen-Deficient *Arabidopsis* Roots. *Plant J.* **2006**, *48*, 522–534. [[CrossRef](#)]
44. Kumar, A.; Silim, S.N.; Okamoto, M.; Siddiqi, M.Y.; Glass, A.D.M. Differential Expression of Three Members of the *AMT1* Gene Family Encoding Putative High-Affinity NH_4^+ Transporters in Roots of *Oryza sativa* Subspecies Indica. *Plant Cell Environ.* **2003**, *26*, 907–914. [[CrossRef](#)]
45. Camañes, G.; Cerezo, M.; Primo-Millo, E.; Gojon, A.; García-Agustín, P. Ammonium Transport and CitAMT1 Expression Are Regulated by N in Citrus Plants. *Planta* **2008**, *229*, 331. [[CrossRef](#)]
46. You, S.; Wang, Y.; Li, Y.; Li, Y.; Tan, P.; Wu, Z.; Shi, W.; Song, Z. Cloning and Functional Determination of Ammonium Transporter PpeAMT3;4 in Peach. *BioMed Res. Int.* **2020**, *2020*, e2147367. [[CrossRef](#)] [[PubMed](#)]
47. Wei, W.; Hu, B.; Li, A.; Chu, C. NRT1.1 in Plants: Functions beyond Nitrate Transport [Cover Story]. *J. Exp. Bot.* **2020**, *71*, 4373–4379. [[CrossRef](#)]
48. Zhang, L.; Yu, Z.; Xu, Y.; Yu, M.; Ren, Y.; Zhang, S.; Yang, G.; Huang, J.; Yan, K.; Zheng, C.; et al. Regulation of the Stability and ABA Import Activity of NRT1.2/NPF4.6 by CEPR2-Mediated Phosphorylation in *Arabidopsis*. *Mol. Plant* **2021**, *14*, 633–646. [[CrossRef](#)]
49. Morère-Le Paven, M.-C.; Viau, L.; Hamon, A.; Vandecasteele, C.; Pellizzaro, A.; Bourdin, C.; Laffont, C.; Lapied, B.; Lepetit, M.; Frugier, F.; et al. Characterization of a Dual-Affinity Nitrate Transporter MtNRT1.3 in the Model Legume *Medicago truncatula*. *J. Exp. Bot.* **2011**, *62*, 5595–5605. [[CrossRef](#)]
50. Yuan, J.-Z.; Cui, Y.-N.; Li, X.-T.; Wang, F.-Z.; He, Z.-H.; Li, X.-Y.; Bao, A.-K.; Wang, S.-M.; Ma, Q. ZxNPF7.3/NRT1.5 from the Xerophyte *Zygophyllum Xanthoxylum* Modulates Salt and Drought Tolerance by Regulating NO_3^- , Na^+ and K^+ Transport. *Environ. Exp. Bot.* **2020**, *177*, 104123. [[CrossRef](#)]
51. Li, J.-Y.; Fu, Y.-L.; Pike, S.M.; Bao, J.; Tian, W.; Zhang, Y.; Chen, C.-Z.; Zhang, Y.; Li, H.-M.; Huang, J.; et al. The *Arabidopsis* Nitrate Transporter NRT1.8 Functions in Nitrate Removal from the Xylem Sap and Mediates Cadmium Tolerance. *Plant Cell* **2010**, *22*, 1633–1646. [[CrossRef](#)]
52. Nour-Eldin, H.H.; Andersen, T.G.; Burow, M.; Madsen, S.R.; Jørgensen, M.E.; Olsen, C.E.; Dreyer, I.; Hedrich, R.; Geiger, D.; Halkier, B.A. NRT/PTR Transporters Are Essential for Translocation of Glucosinolate Defence Compounds to Seeds. *Nature* **2012**, *488*, 531–534. [[CrossRef](#)] [[PubMed](#)]
53. Zhao, X.; Zhang, X.; Liu, Z.; Lv, Y.; Song, T.; Cui, J.; Chen, T.; Li, J.; Zeng, F.; Zhan, Y. Comparing the Effects of N and P Deficiency on Physiology and Growth for Fast- and Slow-Growing Provenances of *Fraxinus mandshurica*. *Forests* **2021**, *12*, 1760. [[CrossRef](#)]
54. El-Gebali, S.; Mistry, J.; Bateman, A.; Eddy, S.R.; Luciani, A.; Potter, S.C.; Qureshi, M.; Richardson, L.J.; Salazar, G.A.; Smart, A.; et al. The Pfam Protein Families Database in 2019. *Nucleic Acids Res.* **2019**, *47*, D427–D432. [[CrossRef](#)] [[PubMed](#)]
55. Finn, R.D.; Clements, J.; Eddy, S.R. HMMER Web Server: Interactive Sequence Similarity Searching. *Nucleic Acids Res.* **2011**, *39*, W29–W37. [[CrossRef](#)]
56. Artimo, P.; Jonnalagedda, M.; Arnold, K.; Baratin, D.; Csardi, G.; de Castro, E.; Duvaud, S.; Flegel, V.; Fortier, A.; Gasteiger, E.; et al. ExpASY: SIB Bioinformatics Resource Portal. *Nucleic Acids Res.* **2012**, *40*, W597–W603. [[CrossRef](#)]

57. Chou, K.-C.; Shen, H.-B. Cell-PLoc 2.0: An Improved Package of Web-Servers for Predicting Subcellular Localization of Proteins in Various Organisms. *Nat. Sci.* **2010**, *2*, 1090. [[CrossRef](#)]
58. Rhee, S.Y.; Beavis, W.; Berardini, T.Z.; Chen, G.; Dixon, D.; Doyle, A.; Garcia-Hernandez, M.; Huala, E.; Lander, G.; Montoya, M.; et al. The *Arabidopsis* Information Resource (TAIR): A Model Organism Database Providing a Centralized, Curated Gateway to *Arabidopsis* Biology, Research Materials and Community. *Nucleic Acids Res.* **2003**, *31*, 224–228. [[CrossRef](#)]
59. Kumar, S.; Stecher, G.; Tamura, K. MEGA7: Molecular Evolutionary Genetics Analysis Version 7.0 for Bigger Datasets. *Mol. Biol. Evol.* **2016**, *33*, 1870–1874. [[CrossRef](#)]
60. Subramanian, B.; Gao, S.; Lercher, M.J.; Hu, S.; Chen, W.-H. Evolvview v3: A Webserver for Visualization, Annotation, and Management of Phylogenetic Trees. *Nucleic Acids Res.* **2019**, *47*, W270–W275. [[CrossRef](#)]
61. Bailey, T.L.; Boden, M.; Buske, F.A.; Frith, M.; Grant, C.E.; Clementi, L.; Ren, J.; Li, W.W.; Noble, W.S. MEME Suite: Tools for Motif Discovery and Searching. *Nucleic Acids Res.* **2009**, *37*, W202–W208. [[CrossRef](#)] [[PubMed](#)]
62. Chen, C.; Chen, H.; Zhang, Y.; Thomas, H.R.; Frank, M.H.; He, Y.; Xia, R. TBtools: An Integrative Toolkit Developed for Interactive Analyses of Big Biological Data. *Mol. Plant* **2020**, *13*, 1194–1202. [[CrossRef](#)] [[PubMed](#)]
63. Wang, Y.; Li, J.; Paterson, A.H. MCScanX-Transposed: Detecting Transposed Gene Duplications Based on Multiple Colinearity Scans. *Bioinformatics* **2013**, *29*, 1458–1460. [[CrossRef](#)] [[PubMed](#)]
64. Lescot, M.; Déhais, P.; Thijs, G.; Marchal, K.; Moreau, Y.; Van de Peer, Y.; Rouzé, P.; Rombauts, S. PlantCARE, a Database of Plant Cis-Acting Regulatory Elements and a Portal to Tools for in Silico Analysis of Promoter Sequences. *Nucleic Acids Res.* **2002**, *30*, 325–327. [[CrossRef](#)] [[PubMed](#)]
65. Szklarczyk, D.; Morris, J.H.; Cook, H.; Kuhn, M.; Wyder, S.; Simonovic, M.; Santos, A.; Doncheva, N.T.; Roth, A.; Bork, P.; et al. The STRING Database in 2017: Quality-Controlled Protein–Protein Association Networks, Made Broadly Accessible. *Nucleic Acids Res.* **2017**, *45*, D362–D368. [[CrossRef](#)]
66. Zhu, K.; Fan, P.; Mo, Z.; Tan, P.; Feng, G.; Li, F.; Peng, F. Identification, Expression and Co-Expression Analysis of R2R3-MYB Family Genes Involved in Graft Union Formation in Pecan (*Carya illinoensis*). *Forests* **2020**, *11*, 917. [[CrossRef](#)]
67. Livak, K.J.; Schmittgen, T.D. Analysis of Relative Gene Expression Data Using Real-Time Quantitative PCR and the $2^{-\Delta\Delta CT}$ Method. *Methods* **2001**, *25*, 402–408. [[CrossRef](#)]
68. Bräutigam, A.; Gagneul, D.; Weber, A.P.M. High-Throughput Colorimetric Method for the Parallel Assay of Glyoxylic Acid and Ammonium in a Single Extract. *Anal. Biochem.* **2007**, *362*, 151–153. [[CrossRef](#)]
69. Patterson, K.; Cakmak, T.; Cooper, A.; Lager, I.; Rasmusson, A.G.; Escobar, M.A. Distinct Signalling Pathways and Transcriptome Response Signatures Differentiate Ammonium- and Nitrate-Supplied Plants. *Plant Cell Environ.* **2010**, *33*, 1486–1501. [[CrossRef](#)]
70. Ogawa, T.; Fukuoka, H.; Yano, H.; Ohkawa, Y. Relationships between Nitrite Reductase Activity and Genotype-Dependent Callus Growth in Rice Cell Cultures. *Plant Cell Rep.* **1999**, *18*, 576–581. [[CrossRef](#)]